

REPORT



Heparin chromatography as an *in vitro* predictor for antibody clearance rate through pinocytosis

Thomas E. Kraft ^a, Wolfgang F. Richter^b, Thomas Emrich ^a, Alexander Knaupp^a, Michaela Schuster ^a, Andreas Wolfert ^a, and Hubert Kettenberger^a

^aRoche Pharma Research and Early Development, Roche Innovation Center Munich, Penzberg, Germany; ^bRoche Pharma Research and Early Development, Roche Innovation Center Basel, Basel, Switzerland

ABSTRACT

The pharmacokinetic (PK) properties of therapeutic antibodies directly affect efficacy, dose and dose intervals, application route and tissue penetration. In indications where health-care providers and patients can choose between several efficacious and safe therapeutic options, convenience (determined by dosing interval or route of application), which is mainly driven by PK properties, can affect drug selection. Therapeutic antibodies can have greatly different PK even if they have identical Fc domains and show no target-mediated drug disposition. Biophysical properties like surface charge or hydrophobicity, and binding to surrogates for high abundant off-targets (e.g., baculovirus particles, Chinese hamster ovary cell membrane proteins) were proposed to be responsible for these differences. Here, we used heparin chromatography to separate a polyclonal mix of endogenous human IgGs (IVIg) into fractions that differ in their PK properties. Heparin was chosen as a surrogate for highly negatively charged glycolyx components on endothelial cells, which are among the main contributors to nonspecific clearance. By directly correlating heparin retention time with clearance, we identified heparin chromatography as a tool to assess differences in unspecific cell–surface interaction and the likelihood for increased pinocytotic uptake and degradation. Building on these results, we combined predictors for FcRn-mediated recycling and cell–surface interaction. The combination of heparin and FcRn chromatography allow identification of antibodies with abnormal PK by mimicking the major root causes for fast, non-target-mediated, clearance of therapeutic, Fc-containing proteins.

ARTICLE HISTORY

Received 4 July 2019
Revised 3 October 2019
Accepted 18 October 2019

KEYWORDS

Pharmacokinetics; neonatal Fc receptor; FcRn; pinocytosis; clearance; prediction; heparin

Introduction

Monoclonal antibodies (mAbs) represent an important class of therapeutics used in a wide variety of diseases.¹ Advanced antibody engineering techniques allow not only humanization and potency optimization, but also the creation of next-generation biotherapeutics such as antibody–drug conjugates, as well as bi- and multi-specific antibodies. This expands the target space and mechanisms of action of the molecules, yielding therapeutic proteins with enhanced functionality. The most prevalent isotype of therapeutic antibody is immunoglobulin G (IgG). A striking feature of IgGs is their comparatively long *in vivo* half-life (about 23 days), which often allows long dose intervals. Long half-life is the result of IgGs binding to the neonatal Fc receptor (FcRn), which efficiently, albeit not perfectly, protects antibodies from lysosomal degradation. If target-mediated clearance (or target-mediated drug disposition, TMDD) can be neglected, antibodies are generally eliminated through pinocytotic uptake by endothelial cells and immune cells (monocytes, macrophages).^{2,3} Pinocytotic uptake is an unspecific process with high turnover rates by which essentially all extracellular components are internalized into endosomes. The endothelial pinocytosis rate has been estimated at 50 nL/h per 10⁶ cells. With an estimated number

of 6.2×10^{11} endothelial cells per person, an endocytotic whole body rate of about 0.75 L/d is expected.^{4,5}

Taking into account the additional contribution by hemopoietic cells,⁶ the total pinocytosis rate is expected to be even higher. Pinocytotic uptake is followed by endosomal sorting and degradation for most serum proteins.⁷ Binding to FcRn at low endosomal pH, however, protects antibodies (and serum albumin) from degradation, leads to efficient recycling and consequently to prolonged serum half-life. For a human IgG, the serum half-life is around 23 days, which is about 10-fold longer than for IgE or IgD, which have a similar size but do not bind to FcRn.⁸ Importantly, the pharmacokinetic (PK) clearance of therapeutic antibodies was shown to span a wide range,^{9,10} even if such antibodies contain the same Fc domain and their PK is not influenced by TMDD.

FcRn-mediated recycling can be improved by engineering the Fc–FcRn binding properties, which has been shown to result in a reduced clearance and prolonged half-life *in vivo*.^{11–14} Efficient FcRn-mediated antibody recycling relies on a delicate balance between binding at low endosomal pH and immediate release/non-binding at serum pH.^{15,16} Residual binding at serum pH may be a result of interactions between the constant or the variable antibody domains with FcRn.^{11–13,17,18} nonspecific

CONTACT Hubert Kettenberger  hubert.kettenberger@roche.com  Roche Pharma Research and Early Development, Roche Innovation Center Munich, Penzberg, Germany.

 Supplemental data for this article can be accessed on the [publisher's website](#).

© 2019 The Author(s). Published with license by Taylor & Francis Group, LLC.

This is an Open Access article distributed under the terms of the Creative Commons Attribution-NonCommercial License (<http://creativecommons.org/licenses/by-nc/4.0/>), which permits unrestricted non-commercial use, distribution, and reproduction in any medium, provided the original work is properly cited.

factors such as charge and hydrophobicity-related interactions or polyreactivity in general have been discussed widely to explain differences in FcRn binding and mAb PK.^{19–23} In the context of charge-mediated differences in PK, features such as isoelectric point (pI), charge and charge distribution have been proposed as the key biophysical features.^{20,23,24}

Charge-mediated interactions can be connected to impaired release from FcRn, but also to unspecific interactions with cell surfaces triggering increased pinocytosis. Vascular endothelial cells, and to a lesser extent also other antibody-degrading cells such as monocytes and macrophages, are coated with a strongly negatively charged glycocalyx, comprising, among other constituents, large amounts of negatively charged oligosaccharides such as heparan and heparin sulfates.²⁵ It is estimated that the complete vascular endothelia of a human spans an area of ~750 m².⁴ Excessive binding to these cell-surface structures may increase the likelihood of pinocytotic uptake and consequently lead to faster proteolytic degradation. The binding to highly abundant cell surface or extracellular matrix structures (nonspecific binding or polyreactivity) has been proposed to be a major driver for antibody PK differences.^{10,21} This led to the development of various assays to detect and quantify these weak, transient interactions. Probes such as Baculovirus particles,⁹ Chinese hamster ovary (CHO) cell membrane proteins,²⁶ human embryonic kidney (HEK) cells, and immobilized heparin²¹ were proposed for such interaction assays. These approaches help explain why differences in FcRn binding alone cannot sufficiently describe differences in antibody PK.^{10,21}

State-of-the-art drug discovery technologies allow the generation and screening of a large number of lead molecules, but experimental determination of PK properties through *in vivo* studies is limited to a small number of candidates for practical and ethical reasons. For the development of new successful biotherapeutics, methods to predict the factors that eventually govern the PK of such proteins are of vital importance. Traditional FcRn interaction assays, e.g., direct binding via surface plasmon resonance (SPR) or biolayer interferometry (BLI), assess FcRn affinity but have difficulty capturing the very weak affinity and fast dissociation rates from FcRn at extracellular pH. Correlating one of the SPR or BLI readouts with actual PK remains a challenging task.²⁷ In contrast, FcRn affinity chromatography mimics the release process at gradually increasing pH on a column. This allows repeated bind and release events over the length of the column and provides an opportunity for resolving small differences in the FcRn dissociation mechanism.

Heparin chromatography offers a way to quantify the second major contributor for antibody PK, namely unspecific, mainly charge-based glycocalyx interaction. Here, we report the use of heparin affinity chromatography as a sensitive, high-resolution tool to separate therapeutic proteins according to their weak unspecific heparin interactions. Using intravenous immunoglobulin (IVIG) as a model substance for a polyclonal, naturally occurring, multi-donor, human antibody repertoire, we show that these polyclonal IgGs, albeit having very similar FcRn binding properties, can be separated by heparin chromatography into

fractions with significant differences in clearance in wild-type, human FcRn transgenic, and FcRn knock-out mice. We further report FcRn and heparin binding data for 131 antibodies that are either marketed or in clinical development, and show that most of them fall into a narrow range of heparin and FcRn interaction strength. The combination of FcRn and heparin chromatography, therefore, provides a way to reliably predict the non-TMDD portion of antibody clearance. The main purpose of this assay combination is the elimination of antibody lead candidates with potentially poor PK properties during the lead selection process, thereby reducing the likelihood of project delays or even failure due to PK liabilities.

Results

Heparin chromatography as a predictor of antibody pinocytosis

IVIG is a preparation of human-derived polyclonal antibodies typically isolated from a pool of >1000 donors. The IgG subclasses match those in normal human serum. IVIG contains about 22% of a high-molecular-weight (HMW) (mostly dimer) fraction, which is attributed to anti-idiotypic antibody pairs (i.e., antibodies that bind to other antibodies in this multi-donor preparation) or otherwise dimerization-prone antibodies. For the experiments described in this study, the HMW fraction was removed via preparative size-exclusion chromatography (SEC). The resulting monomer fraction was then subjected to heparin affinity chromatography and separated into three fractions with short, medium and long retention times on a salt gradient (see Materials and Methods).

Under low-salt conditions, heparin chromatography retains antibodies even if their affinity to heparin is very small. Salt-gradient elution then separates antibodies according to differences in their binding behavior. In contrast to direct interaction methods such as SPR or ELISA-type assays, there are many subsequent binding and release events along the chromatography column that collectively contribute to the resolving power of this method. Moreover, chromatography is a facile, well-established, and robust method that can be used both for analytical and preparative purposes.

If heparin affinity (as a surrogate readout for cell-surface binding) plays a significant role in antibody PK, weak and strong-binding heparin chromatography fractions of IVIG should show a difference in PK *in vivo*. To test this hypothesis, we generated three fractions of IVIG, namely fraction 1 (no heparin binding), fraction 2 (the peak fraction) and fraction 3 (the long late-eluting tail, which comprises approximately 5% of IVIG) (Figure 1). Successful partitioning into different heparin binding fractions was confirmed by analytical heparin chromatography (Figure 2B). Moreover, an isoelectric focusing gel showed that the fractions differ notably in their mean pI (Figure S1). Further characterization of these fractions by SEC and capillary electrophoresis shows that all three fractions show a comparably high degree of homogeneity, monomer content and a consistently low amount of fragmentation (Figure S2).

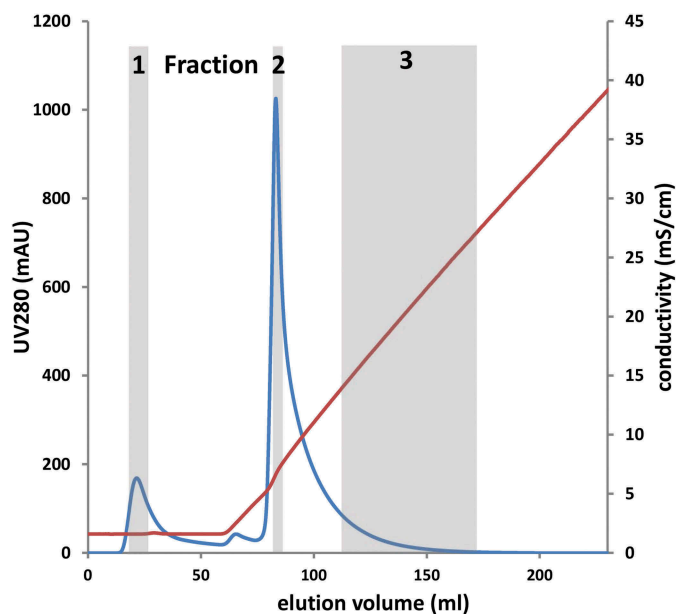


Figure 1. IVIG fractionation on a preparative heparin column. The blue trace shows the UV absorption at 280 nm; the red trace indicates conductivity. Gray areas indicate where fractions 1, 2 and 3, respectively, were collected.

IVIG shows a narrow distribution on FcRn affinity chromatography

FcRn affinity chromatography is a simple and sensitive mimic for the dissociation behavior of antibodies when endosomal vesicles re-appear at the cell surface. In this assay, samples are bound to a chromatographic resin at low pH (pH 5.5) and eluted with a pH gradient up to pH 8.0. Antibodies elute at retention times that reflect their release behavior during the pH switch from endosomal to extracellular pH. Antibodies showing impaired release at extracellular pH have an increased likelihood to remain bound to the cell surface, and thus have a higher risk to undergo another round of pinocytosis. As described above,

each pinocytosis event has a certain likelihood to end in the degrading lysosomes, which negatively impacts *in vivo* PK.

The unfractionated and heparin-fractionated IVIG samples were subjected to FcRn affinity chromatography as described previously.^{28,29} Surprisingly, the peak widths, i.e., the distribution of FcRn retention times for all samples, were identical and nearly as narrow as for a purified mAb (Figure 2). We used briakinumab and ustekinumab as controls in this experiments because these two mAbs flank a wide range of FcRn retention times.²⁸ The narrow retention time distribution of IVIG suggests that the abundant naturally occurring antibodies are found in IVIG are selected by nature for very defined FcRn interaction properties, despite being very diverse in their variable domains.

The pharmacokinetics of IVIG fractions in three different mouse models

In order to test the hypothesis of a correlation between heparin binding and *in vivo* PK, we determined the clearance of the IVIG heparin fractions after single intravenous injections into three different mouse strains. Wild-type FcRn mice (strain C57BL/6) have normal levels of murine FcRn. Human IgG1 shows a higher affinity to murine FcRn than the endogenous mouse IgG.^{30–32} Therefore, the injected human antibodies can outcompete endogenous mouse IgG. The mouse strain tg32 is homozygous for human FcRn and bears a homozygous murine FcRn knock-out. It serves as a model for human FcRn-mediated antibody turnover. Endogenous mouse IgG does not interact significantly with human FcRn.^{30–32} Consequently, this mouse strain shows decreased murine IgG levels due to poor FcRn-mediated recycling. The third mouse strain was mice lacking the mFcRn α -chain (B6.129 x 1-Fcgrt^{tm1Dcr}/DcrJ) and is referred to as FcRn ko. Due to the absence of FcRn-mediated sorting and recycling in these mice, the PK of antibodies is essentially dominated by

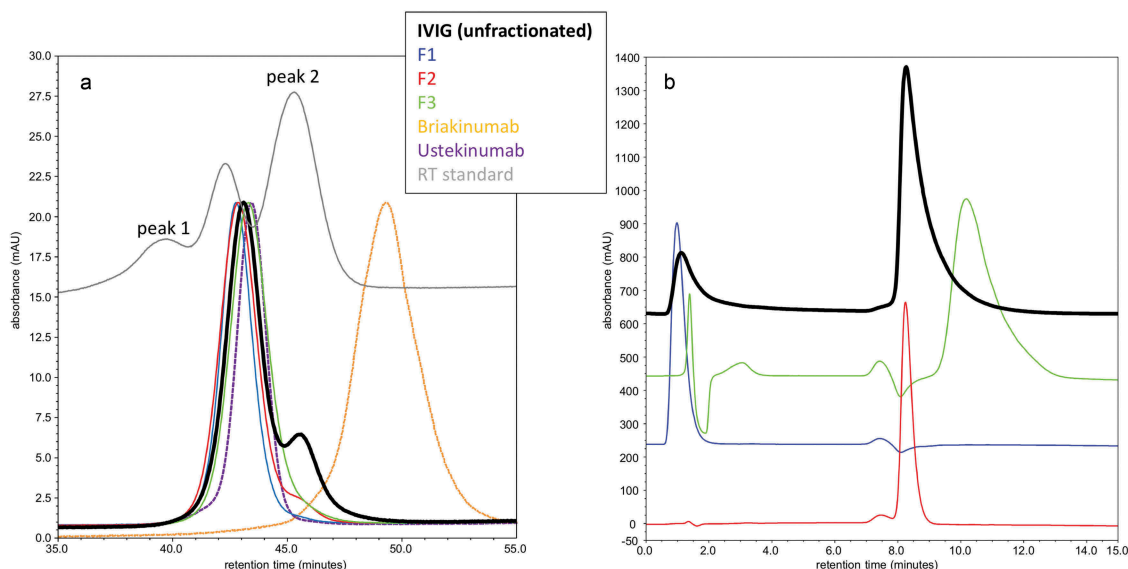


Figure 2. (A) Retention of IVIG fractions and control samples on hFcRn column; peaks 1 and 2 of the retention time standard, which are used for the calculation of the relative retention time, are indicated. Briakinumab and ustekinumab are shown as examples for unusually strong and “typical” examples, respectively. (B) Re-chromatography of IVIG fractions by analytical heparin HPLC.

pinocytosis followed by lysosomal degradation. Clearance should, therefore, be a direct metric for the extent of pinocytotic IgG uptake, which is irreversible due to lack of FcRn-mediated salvage.

Confirming our hypothesis that heparin retention can serve as metric for pinocytosis rate of IgGs, we found a more than two-fold higher clearance of the high heparin affinity fraction 3 compared to the low heparin affinity fraction 1 in the FcRn ko mouse model (Figure 2A). This may be attributed to enhanced pinocytotic uptake of IgGs with strong binding to the heparin column. Fraction 2 was cleared at an intermediate rate compared to fractions 1 and 3. In both the FcRn wild-type and the human FcRn transgenic mouse strains, differences of clearance between fractions 1, 2 and 3 were smaller, with a trend toward faster clearance/shorter terminal half-life of fraction 3 (Figure 3 and Supplementary Table 1).

Combining predictors for pinocytosis and FcRn recycling

In previous studies, it was shown that FcRn binding at low pH and release at neutral pH plays an important role for antibody PKs.^{7,10,21,22,28,29,33,34} Specifically, IgG retention to column-immobilized FcRn, bound at low pH followed by elution using a pH gradient, correlated with terminal half-lives *in vivo* for a set of related mAbs.^{28,29} However, FcRn binding alone is not sufficient to reliably predict PK. Conducting mouse PK studies with heparin-fractionated endogenous human polyclonal antibodies (IVIG), we demonstrated that binding on the negatively charged heparin column alone can be indicative of significant difference in clearance, even for samples with identical FcRn binding characteristics. We

therefore investigated if a combination of the heparin and FcRn column assays can improve the predictivity for *in vivo* PK *in vitro*.

In order to validate this assay combination, we determined the heparin and FcRn column retention times of 41 internal mAbs and bispecific antibodies with known clearance in cynomolgus monkeys (Figure 4A). Only molecules that did not show TMDD or anti-drug antibody formation were included in the analysis. Clearance values were categorized into four categories (fast: >12 mg/kg/day; intermediate: clearance between 8 and 12 mg/kg/day, slow: clearance between 8 and 2.5 ml/kg/day, and very slow: clearance <2.5 mL/kg/day). Based on these data, a window of heparin and FcRn column retention times can be defined, which allows the prediction of slow/intermediate vs. fast clearance. In the dataset we studied, 90% of the antibodies within this “good PK” window (28 of 30) and 74% of the antibodies outside the window (14 of 19) were categorized correctly. We purposefully set stringent criteria, i.e., a small window in order to decrease the likelihood of falsely categorizing antibodies with fast clearance while accepting the possibility of incorrectly predicting the clearance of slow-clearing antibodies. Interestingly, many of the fast-clearing compounds are bispecific antibodies. While we do not yet understand the reasons for their fast clearance, the heparin/FcRn chromatography combination is able to capture and correctly predict this fast clearance, irrespective of the actual antibody format.

To further characterize the capability of this prediction method, we tested a set of immunoglobulins that comprise the variable regions of 131 clinical-stage antibodies in the heparin and FcRn column retention assays (Supplementary Table 2). These variable domains were grafted on a common

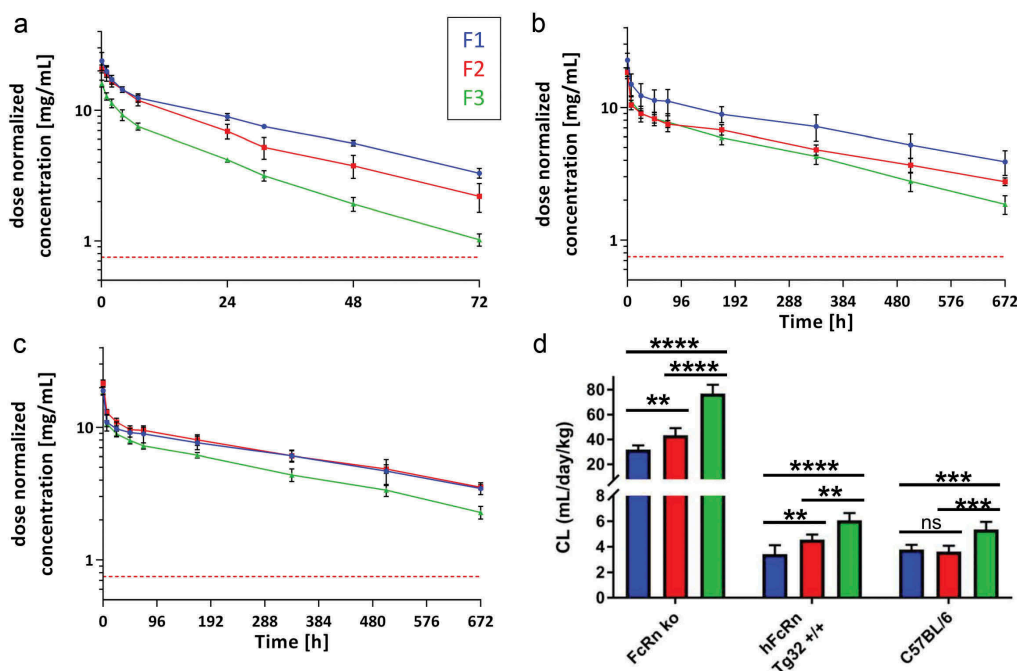


Figure 3. Serum concentration vs. time profiles for fractions 1, 2 and 3. (A) FcRn ko mice. (B) hFcRn Tg32 homozygous mice. (C) wild-type (C57BL/6) mice. (D) Clearance of IVIG fractions in the different mouse models. Clearance values represent the mean \pm S.D. of five mice per experiment. The red-dotted line marks the assay detection limit. Asterisks denote statistically significant differences (** $p \leq 0.01$, *** $p \leq 0.001$, **** $p \leq 0.0001$) as determined by one-way ANOVA plus a posteriori Holm-Sidak test.

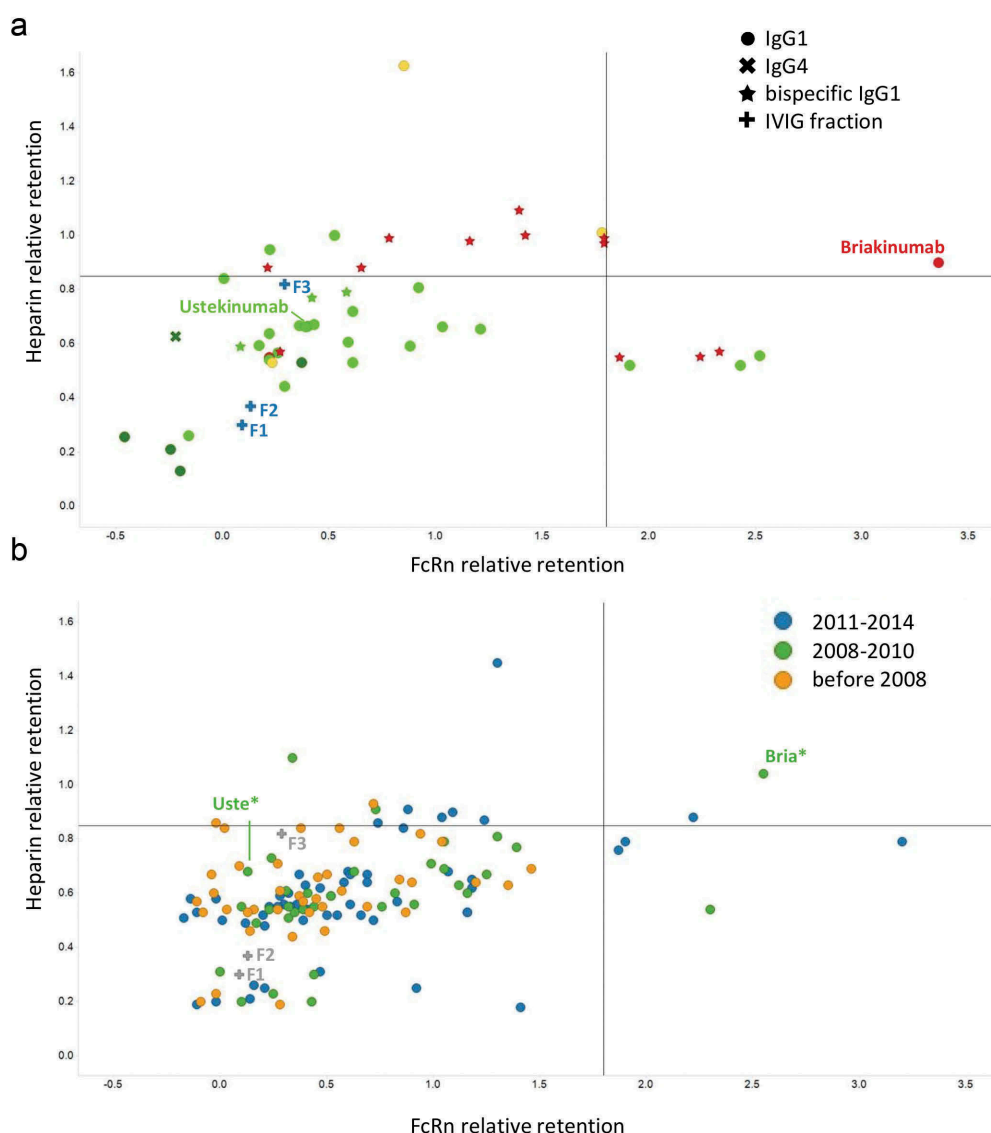


Figure 4. (A) Correlation of heparin and FcRn column retention for Roche clinical candidates colored according to qualitative clearance in cynomolgus monkeys (dark green, very slow, <2.5 mL/kg/day; green, slow, <8 mL/kg/day; yellow, intermediate >8 and <12 mL/kg/day; red >12 mL/kg/day). (B) Heparin and FcRn column retention of antibodies from Jain et al.³⁵ Heparin and FcRn binding data were generated as part of this study. The color code reflects the year in which the INN was first assigned. Uste* and Bria* denotes the variable domains of briakinumab and ustekinumab on a common IgG1 constant region.

Cutoffs were chosen manually to separate mAbs with fast and normal clearance. IVIG fractions F1, F2, and F3 were added for comparison.

IgG1 Fc domain, transiently expressed in HEK cell culture and kindly provided by the authors of a previous study of these 131 molecules.³⁵ This set of molecules is meant to span a sequence variety encountered in currently investigated therapeutic antibodies. Of this set, 87% (115 of 131) show FcRn and heparin retention times that fall into the slow/intermediate PK window, indicating that sufficiently low heparin binding and sufficiently efficient FcRn release is characteristic for most clinical-stage antibodies. Assuming that more recent projects (i.e., antibodies in Phase 1 and 2 clinical trials) were generally developed with better understanding of antibody PK, it can be observed that 91% of the Phase 1 or 2 molecules (42 of 46) fall within the low heparin and low FcRn binding window. These results further validate our approach of combining the heparin and FcRn column as an *in vitro* prediction

tool for mAbs, and provide arguments for applying this window to new lead molecules (Figure 4B).

Discussion

In contrast to small molecules, antibody serum clearance is not mainly governed by hepatic metabolism and renal excretion but by intracellular degradation. Major processes influencing the IgG clearance are nonspecific uptake into endothelial and hematopoietic cells via fluid-phase pinocytosis and FcRn mediated recycling. Much of the available literature has focused on FcRn mediated recycling as a key driver for differential antibody clearance rates. Here, we focus on the other main component of clearance, fluid-phase pinocytosis, to explain differences in antibody PK and to develop an assay that captures them.

Based on reported PK differences of antibodies that differ in their Fv charge, we hypothesized that these differences are caused by nonspecific binding of the antibody to the glycocalyx of endothelial cells, thereby affecting the pinocytosis rate. In order to test this hypothesis, we used antibody retention to column-immobilized heparin as a surrogate for the glycocalyx interaction, affecting pinocytosis rate as a driver for clearance. IVIG was selected as a model system for therapeutic IgGs because it contains a vast repertoire of highly different human antibodies from multiple donors. Testing of IVIG fractions drastically reduced the number of samples to be tested compared to mAbs, as each IVIG fraction contains a huge number of IgGs with diverse sequences that share a similar heparin column retention behavior.

Strikingly, IVIG shows a narrow distribution of FcRn binding, i.e., FcRn affinity column retention time. The FcRn column peak width of IVIG is nearly as narrow as for purified mAbs (Figure 2A), indicating that FcRn binding, and thus FcRn-mediated recycling, is tightly controlled by nature. Interestingly, mAbs developed for therapeutic use span a wide range in FcRn column retention (Figure 4). This finding reflects in part the large differences in clearance of therapeutic antibodies compared to endogenous ones.

In contrast to FcRn, IVIG heparin retention spans a wider range (Figure 1). Heparin, as a poly-anionic ligand, can separate antibodies according to their ability to directly interact with heparin, but mainly according to their charge properties. We determined the differences in pI distributions of the three IVIG heparin fractions reported in this study by isoelectric focusing (Supplementary Figure S1) and found a correlation between heparin retention and pI. MAbs have been found to cover a wider range of heparin retention than IVIG, especially toward higher retention times. IVIG represents a mixture of “typical” and predominantly long-lived human immunoglobulins. We assume that antibodies with fast clearance should be under-represented in IVIG preparations because, in such cases, clearance would counter-balance production. Since antibodies with fast clearance are expected to be under-represented in IVIG, we aimed at isolating the extreme tail (fraction 3), i.e., the fraction comprising about 5% of the strongest heparin binders in order to also cover this range.

Confirming our hypothesis that heparin retention can serve as a measurement for fluid-phase pinocytosis, the IVIG fraction with the lowest heparin retention (fraction 1) showed the lowest clearance, and therefore the lowest pinocytosis rate in FcRn knock-out mice (Figure 3). In these mice, every pinocytotic event generally leads to the degradation of the pinocytosed IgG. Therefore, differences in clearance can be directly correlated with differences in pinocytosis rate, making these mice an excellent model for studying the pinocytosis behavior of different therapeutic antibodies *in vivo*. IVIG fractions 2 and 3, which were selected for their increased heparin retention, also showed an increase in clearance in this mouse model, accordingly. Wild-type (C57BL/6J) mice showed a less pronounced difference between heparin fractions of IVIG (Figure 3C). The expression of only murine FcRn in this mouse strain, which shows markedly higher affinity to hIgGs compared to human FcRn,^{36–39} could explain this observation. The C57BL/6J mouse model is not ideal to predict IgG clearance in humans because it overestimates the

contribution of FcRn to IgG recycling.⁴⁰ To test whether this correlation still holds true in a model with high predictive power for human antibody PK,⁴⁰ we determined the clearance in hFcRn Tg32 homozygous mice. Similar to FcRn knock-out mice, this mouse model also showed a direct correlation of clearance with heparin retention. Considering the near-identical retention time of the three IVIG fractions on the FcRn column (Figure 2A), it is most likely that the difference in clearance did not arise from varying FcRn recycling, thus strengthening our confidence in the predictive power of the heparin column for nonspecific antibody clearance in humans, mediated via pinocytosis.

Mimicking the two major processes of nonspecific IgG clearance, i.e., pinocytosis and FcRn-mediated recycling, we combined the retention of the heparin and the FcRn column in order to achieve greater predictivity of antibody clearance (Figure 4). By defining a threshold in both dimensions, we separated molecules with clearance in cynomolgus monkeys in the typical range (<12 ml/day/kg) from antibodies with atypical PK with 90% of the molecules in the “good PK” window being categorized correctly. We set a stringent cutoff to exclude fast-clearing antibodies from the development process with high probability, even at the cost of falsely flagging a slow-clearing antibody. Our rationale was to be able to advance molecules within the “good PK” window quickly from the lead identification to optimization phase without an *in vivo* PK study, which we only deemed necessary at this stage as a confirmatory measurement for molecules that received a heparin-FcRn column PK flag. We gained further confidence in the predictive power of flagging fast-clearing molecules through this assay combination by testing a set of 131 clinical-stage therapeutic antibodies (all on a common IgG1 Fc).³⁵ These antibodies, especially those in earlier stages, have undergone PK evaluation before entering clinical phase. Furthermore, the majority of molecules with PK properties that were prohibitive for their therapeutic or commercial success were most likely not developed to this point, and would therefore be missing from this dataset. Thus, it is expected that most of these antibodies should have PK properties that are compatible with clinical development; however, consistent and comparable PK data for this set of antibodies are not available in the literature. We found that 87% of the clinical-stage molecules fall within the “good PK” window of heparin and FcRn column retention, confirming the applicability of this assay for antibodies originating from various development backgrounds. Heparin and FcRn chromatography represent additional characterization parameters that are essentially uncorrelated to commonly used biophysical readouts addressing hydrophobicity and self-interaction (Figure S3). A weak correlation was only observed between FcRn relative retention and the cross-interaction chromatography retention time³⁵ and affinity capture-self-interaction nanoparticle spectroscopy.³⁵

We conclude that the assay combination is most useful as a de-risking tool for fast clearance in early antibody profiling and developability assessment. However, the results are limited to the flagging of fast-clearing compounds, while the assay cannot reliably rank compounds within the slow/intermediate clearance range by PK. Further development of predictive *in vitro* assays is required to add more granularity and rank compounds quantitatively.

Material and methods

Samples

Antibodies shown in [Figure 4A](#) were expressed in-house via transient transfection in HEK293 cells or via stable CHO cell lines and purified with standard techniques to achieve a purity of >90% by SEC. Antibodies shown in [Figure 4B](#) were kindly provided by Adimab and prepared as described previously.³⁵

IVIG fractionation on heparin

IVIG (SUBCUVIA, manufactured by Baxter) monomer and dimer fractions were separated via preparative SEC (HiLoad 26–60 Superdex 200, GE Healthcare) using phosphate-buffered saline running buffer. Fractions containing monomeric IVIG were pooled, followed by buffer exchange to low-salt buffer A (20 mM Tris pH 7.4) using Amicon Ultra 15 (30 kDa MWCO, EMD Millipore) according to the manufacturer's instructions. Five commercially available heparin columns (HiTrap Heparin HP, 5 ml, GE Healthcare) were connected in line and equilibrated with buffer C (20 mM Tris pH 7.4) at a flow rate of 5.0 mL/min. A total of 50 mg monomeric IVIG was injected. Two minutes post-sample application at a flow of 2ml/min, the column was washed with 25 mL of buffer C at a flow rate of 5 mL/min, followed by a linear gradient from 0% to 40% buffer D (20 mM Tris, pH 7.4, 1 M NaCl) over 7 column volumes. The column was re-equilibrated with buffer C. Detection was performed with a UV detector at 280 nm. Fractions of 2 mL were collected and pooled according to [Figure 1](#), buffer exchanged to 20 mM histidine, 140 mM NaCl, pH 6.0, and concentrated using Amicon Ultra 15 (30 kDa MWCO, EMD Millipore) according to the manufacturer's instructions.

Analytical heparin affinity chromatography

Samples were re-buffered in 20 mM histidine, pH 5.5 to reduce ionic strength and ensure complete binding. A commercially available heparin column (TSK-Gel Heparin-5PW 5 × 50 mm, Tosoh Biosciences) was equilibrated with buffer A (50 mM Tris pH 7.4) at a column temperature of 25°C and a flow rate of 0.8 mL/min. A total of 35 µg protein was injected. Two minutes post injection, a linear gradient from 0–55% buffer B (20 mM Tris, pH 7.4, 1 M NaCl) over 16.5 min was started. Buffer B concentration was increased to 100% over 0.5 min and held for 4 min before the column was re-equilibrated with buffer A. Detection was performed with a UV detector set at 220 nm. In order to make results from different runs and different buffer and column lots comparable, relative retention time (t_{rel}) was calculated using a standard sample with a high retention time according to Equation 1:

$$t_{rel} = \frac{t_{sample}}{t_{standard}} \quad (1)$$

with t_{sample} and $t_{standard}$ indicating the retention times of the sample and the standard sample, respectively.

FcRn affinity chromatography

Analytical FcRn affinity chromatography was performed using a commercially available FcRn affinity column (Part No. 08128057001, Roche), pre-equilibrated with 80% buffer A (20 mM MES sodium salt, 140 mM NaCl, pH 5.5) and 20% buffer B (20 mM Tris/HCl, 140 mM NaCl, pH 8.8) at a flow rate of 0.5 mL/min and a column temperature of 25°C. Samples were prepared as above. A total of 30 µg protein was injected. Ten minutes post injection, a linear gradient from 20% to 100% buffer B over 70 min was started. One hundred percent buffer B was held for 10 min before the column was re-equilibrated with 80% buffer A and 20% buffer B. Detection was performed with a UV detector set at 280 nm. In order to make results from different runs and different buffer and column lots comparable, and to compensate for slight retention time drifts, a standard sample was measured at the beginning and the end of each sequence and after every 10th run. The relative retention time (t_{rel}) was calculated according to Equation 2.

$$t_{rel} = \frac{t_{sample} - t_{standardpeak1}}{t_{standardpeak2} - t_{standardpeak1}} \quad (2)$$

Determination of the isoelectric point by isoelectric focusing gel electrophoresis

Heparin fractionized IVIG was dialyzed overnight in 3 mM Tris, pH 3.8. Samples were mixed with Novex™ IEF Sample Buffer pH 3–10 (2X) (ThermoFisher), loaded onto a Novex™ pH 3–10 IEF Protein Gel (ThermoFisher) and run according to the manufacturer's instructions. After staining with Coomassie (SimplyBlue™ SafeStain, ThermoFisher) according to the manufacturer's instructions, the pI of IVIG fraction protein bands were determined by comparison to IEF Marker 3–10 (ThermoFisher).

Size-exclusion chromatography

Samples were separated using a TSK-Gel G3000SWXL column (Tosoh Bioscience) with 0.2 M potassium phosphate, 0.25 M KCl, pH 7.0 as the mobile phase at a flow rate of 0.5 mL/min. A UV detector at 280 nm was used to detect and quantify proteins.

Capillary gel electrophoresis

Protein capillary gel electrophoresis was performed on a Caliper LabChip GXII (Perkin Elmer) according to the manufacturer's instructions.

In vivo experiments and bioanalytics

The study was conducted using female mice lacking the mFcRn α -chain (B6.129 x 1-Fcgrt^{tm1Dcr}/Dcr]; abbreviated mFcRn ko), female B6. Cg-Fcgrt^{tm1Dcr} Tg(FCGRT)32Dcr/Dcr] mice (abbreviated hFcRn Tg32), and female wild-type C57BL/6 mice. hFcRn Tg32 mice carry a knock-out allele of the FcRn α -chain and are homozygous for a human FcRn α -

chain genomic transgene under control of its human promoter.

Mice received a single intravenous injection into the tail vein of the respective IVIG fraction (dose level 5 mg/kg) ($n = 5/\text{dose group}$).

In hFcRn Tg32 and wild-type mice, serial samples of blood (20 μl) were collected from each animal at 5 min, 7, 24, 48, 72 h and then weekly for up to 4 weeks after the injection, and in FcRn ko mice at 5 min, 1, 2, 4, 7, 24, 31, 48, and 72 h. Blood was collected from the tail vein over K3 EDTA as anticoagulant. Plasma was separated by centrifugation and samples were stored at -20°C until analysis. All animal experiments were conducted according to applicable guidelines and approved by Swiss authority. The animal laboratory is AAALAC accredited.

Plasma concentrations of IVIG IgG in murine serum samples were determined by a human IgG-specific electrochemiluminescence immunoassay method. Briefly, plasma samples, pre-diluted with assay buffer, were incubated with capture and detection molecules for 9 min at 37°C . Biotinylated mAb<H-Fc γ -pan>M-IgG was used as capture molecule and a ruthenium(II)tris(bipyridyl) $_3^{2+}$ labeled mAb<H-Fc γ -pan>M-IgG mouse mAb was used for detection. Both antibodies were generated and labeled in-house. Streptavidin-coated magnetic microparticles were added and incubated for additional 9 min at 37°C to allow complex formation due to biotin–streptavidin interactions. Complexes were magnetically captured on an electrode and a chemiluminescent signal generated using the co-reactant tripropylamine was measured by a photomultiplier detector. All plasma samples and positive or negative control samples were analyzed in replicates and calibrated against the administered IVIG heparin fraction using a cubic-parameter fitting model.

The PK parameters were estimated by standard non-compartmental analysis, using the PK evaluation program Phoenix WinNonlin 6.4 (Phoenix[®]). Individual plasma concentration-time profiles were used for parameter estimation.

Acknowledgments

We are very grateful to Max Vásquez, Tushar Jain, Yingda Xu, Laura Walker and Dane Wittrup for sharing samples, and for the valuable discussions and inspirations, we received during the preparation of this manuscript.

Disclosure of potential conflicts of interest

All authors are current employees of Roche.

ORCID

Thomas E. Kraft  <http://orcid.org/0000-0002-5528-3197>
 Thomas Emrich  <http://orcid.org/0000-0003-1179-4697>
 Michaela Schuster  <http://orcid.org/0000-0003-2817-8364>
 Andreas Wolfert  <http://orcid.org/0000-0003-3605-0010>

References

- Elvin JG, Couston RG, van der Walle CF. Therapeutic antibodies: market considerations, disease targets and bioprocessing. *Int J Pharm.* 2013;440:83–98. doi:10.1016/j.ijpharm.2011.12.039.
- Tabrizi M, Tseng C-M RL. Elimination mechanisms of therapeutic monoclonal antibodies. *Drug Discov Today.* 2006;11:81–88. doi:10.1016/S1359-6446(05)03638-X.
- Dostalek M, Gardner I, Gurbaxani BM, Rose RH, Chetty M. Pharmacokinetics, pharmacodynamics and physiologically-based pharmacokinetic modelling of monoclonal antibodies. *Clin Pharmacokinet.* 2013;52:83–124.
- Sender R, Fuchs S, Milo R. Revised estimates for the number of human and bacteria cells in the body. *PLoS Biol.* 2016;14:e1002533. doi:10.1371/journal.pbio.1002533.
- Glassman P, Balthasar J. Physiologically-based pharmacokinetic modeling to predict the clinical pharmacokinetics of monoclonal antibodies. *J Pharmacokinet Phar.* 2016;43:427–46. doi:10.1007/s10928-016-9482-0.
- Richter WF, Christianson GJ, Frances N, Grimm H, Proetz G, Roopenian DC. Hematopoietic cells as site of first-pass catabolism after subcutaneous dosing and contributors to systemic clearance of a monoclonal antibody in mice. *mAbs.* 2018;10:803–13. doi:10.1080/19420862.2018.1458808.
- Gurbaxani B, Dostalek M, Gardner I. Are endosomal trafficking parameters better targets for improving mAb pharmacokinetics than FcRn binding affinity? *Mol Immunol.* 2013;56:660–74. doi:10.1016/j.molimm.2013.05.008.
- Lobo ED, Hansen RJ, Balthasar JP. Antibody pharmacokinetics and pharmacodynamics. *J Pharm Sci.* 2004;93:2645–68. doi:10.1002/jps.20178.
- Hötzel I, Theil F-P-P, Bernstein LJ, Prabhu S, Deng R, Quintana L, Lutman J, Sibia R, Chan P, Bumbaca D, et al. A strategy for risk mitigation of antibodies with fast clearance. *MAbs.* 2012;4:753–60. doi:10.4161/mabs.22189.
- Kelly R, Yu Y, Sun T, Caffry I, Lynaugh H, Brown M, Jain T, Xu Y, Wittrup. Target-independent variable region mediated effects on antibody clearance can be FcRn independent. *mAbs.* 2016;8:1269–75. doi:10.1080/19420862.2016.1208330.
- Igawa T, Tsunoda H, Tachibana T, Maeda A, Mimoto F, Moriyama C, Nanami M, et al. Reduced elimination of IgG antibodies by engineering the variable region. *Protein Eng Des Sel.* 2010;23:385–92. doi:10.1093/protein/gzq009.
- Sampei Z, Igawa T, Soeda T, Okuyama-Nishida Y, Moriyama C, Wakabayashi T, Tanaka E, Muto A, Kojima T, Kitazawa T, et al. Identification and multidimensional optimization of an asymmetric bispecific IgG antibody mimicking the function of factor VIII cofactor activity. *PLoS One.* 2013;8:e57479. doi:10.1371/journal.pone.0057479.
- Wu H, Pfarr DS, Johnson S, Brewah YA, Woods RM, Patel NK, White WI, Young JF, Kiener PA. Development of motavizumab, an ultra-potent antibody for the prevention of respiratory syncytial virus infection in the upper and lower respiratory tract. *J Mol Biol.* 2007;368:652–65. doi:10.1016/j.jmb.2007.02.024.
- Leipold D, Pharmacokinetic PS. Pharmacodynamic Considerations in the design of therapeutic antibodies. *Clin Transl Sci.* 2019;12:130–39. doi:10.1111/cts.12597.
- Maas B, Cao Y. A minimal physiologically based pharmacokinetic model to investigate FcRn-mediated monoclonal antibody salvage: effects of kon, koff, endosome trafficking, and animal species. *Mabs.* 2018;10:1322–31. doi:10.1080/19420862.2018.1506648.
- Chung S, Lin Y, Nguyen V, Kamen L, Zheng K, Vora B, Song A. Development of a label-free FcRn-mediated transcytosis assay for in vitro characterization of FcRn interactions with therapeutic antibodies and Fc-fusion proteins. *J Immunol Methods.* 2018;462:101–05. doi:10.1016/j.jim.2018.07.004.
- Hinton PR, Xiong JM, Johlfs MG, Tang MT, Keller S, Tsurushita N. An engineered human IgG1 antibody with longer serum half-life. *J Immunol.* 2006;176:346–56. doi:10.4049/jimmunol.176.1.346.
- Jensen P, Schoch A, Larraillat V, Hilger M, Schlothauer T, Emrich T, Rand K. A two-pronged binding mechanism of IgG to the neonatal Fc receptor controls complex stability and IgG serum half-life. *Mol Cell Proteomics.* 2017;16:451–56. doi:10.1074/mcp.M116.064675.
- Bumbaca D, Boswell AC, Fielder PJ, Khawli LA. Physicochemical and biochemical factors influencing the pharmacokinetics of

- antibody therapeutics. *Aaps J.* 2012;14:554–58. doi:10.1208/s12248-012-9369-y.
20. Sharma V, Patapoff T, Kabakoff B, Pai S, Hilario E, Zhang B, Li C, Borisov O, Kelley R, Chorny I, et al. In silico selection of therapeutic antibodies for development: viscosity, clearance, and chemical stability. *Proc Natl Acad Sci U S A.* 2014;111:18601–06. doi:10.1073/pnas.1421779112.
 21. Datta-Mannan A, Lu J, Witcher D, Leung D, Tang Y, Wroblewski V. The interplay of non-specific binding, target-mediated clearance and FcRn interactions on the pharmacokinetics of humanized antibodies. *Mabs.* 2015;7:1084–93. doi:10.1080/19420862.2015.1075109.
 22. Datta-Mannan A, Croy J, Schirtzinger L, Torgerson S, Breyer M, Wroblewski V. Aberrant bispecific antibody pharmacokinetics linked to liver sinusoidal endothelium clearance mechanism in cynomolgus monkeys. *mAbs.* 2016;8:969–82. doi:10.1080/19420862.2016.1178435.
 23. Datta-Mannan A, Thangaraju A, Leung D, Tang Y, Witcher D, Lu J, Wroblewski V. Balancing charge in the complementarity-determining regions of humanized mAbs without affecting pI reduces non-specific binding and improves the pharmacokinetics. *Mabs.* 2015;7:483–93. doi:10.1080/19420862.2015.1016696.
 24. Li B, Tesar D, Boswell A, Cahaya H, Wong A, Zhang J, Meng G, Eigenbrot C, Pantua H, Diao J, et al. Framework selection can influence pharmacokinetics of a humanized therapeutic antibody through differences in molecule charge. *mAbs.* 2014;6:1255–64. doi:10.4161/mabs.29809.
 25. Bernfield M, Götte M, Park P, Reizes O, Fitzgerald M, Lincecum J, Zako M. Functions of cell surface heparan sulfate proteoglycans. *Annu Rev Biochem.* 1999;68:729–77. doi:10.1146/annurev.biochem.68.1.729.
 26. Xu Y, Roach W, Sun T, Jain T, Prinz B, Yu T-Y-Y, Torrey J, Thomas J, Bobrowicz P, Vásquez M, et al. Addressing polyspecificity of antibodies selected from an in vitro yeast presentation system: a FACS-based, high-throughput selection and analytical tool. *Protein Eng Des Sel.* 2013;26:663–70. doi:10.1093/protein/gzt047.
 27. Gurbaxani B, Cruz L, Chintalacheruvu K, Morrison S. Analysis of a family of antibodies with different half-lives in mice fails to find a correlation between affinity for FcRn and serum half-life. *Mol Immunol.* 2006;43:1462–73. doi:10.1016/j.molimm.2005.07.032.
 28. Schoch A, Kettenberger H, Mundigl O, Winter G, Engert J, Heinrich J, Emrich T. Charge-mediated influence of the antibody variable domain on FcRn-dependent pharmacokinetics. *Proc National Acad Sci.* 2015;112:5997–6002. doi:10.1073/pnas.1408766112.
 29. Schlothauer T, Rueger P, Stracke J, Hertenberger H, Fingas F, Kling L, Emrich T, Drabner G, Seeber S, Auer J, et al. Analytical FcRn affinity chromatography for functional characterization of monoclonal antibodies. *mAbs.* 2013;5:576–86. doi:10.4161/mabs.24981.
 30. Ober R, Radu C, Ghetie V, Ward S. Differences in promiscuity for antibody–FcRn interactions across species: implications for therapeutic antibodies. *Int Immunol.* 2001;13:1551–59. doi:10.1093/intimm/13.12.1551.
 31. Abdiche Y, Yeung Y, Chaparro-Riggers J, Barman I, Strop P, Chin S, Pham A, Bolton G, McDonough D, Lindquist K, et al. The neonatal Fc receptor (FcRn) binds independently to both sites of the IgG homodimer with identical affinity. *mAbs.* 2015;7:331–43. doi:10.1080/19420862.2015.1008353.
 32. Neuber T, Frese K, Jaehrling J, Jäger S, Daubert D, Felderer K, Linnemann M, Höhne A, Kaden S, Kölln J, et al. Characterization and screening of IgG binding to the neonatal Fc receptor. *mAbs.* 2014;6:928–42. doi:10.4161/mabs.28744.
 33. Borrok J, Wu Y, Beyaz N, Yu X-Q, Oganessian V, Dall’Acqua W, Tsui P. pH-dependent binding engineering reveals an FcRn affinity threshold that governs IgG recycling. *J Bio Chem.* 2015;290:4282–90. doi:10.1074/jbc.M114.603712.
 34. Souders C, Nelson S, Wang Y, Crowley A, Klempner M, Thomas W. A novel in vitro assay to predict neonatal Fc receptor-mediated human IgG half-life. *mAbs.* 2015;7:912–21. doi:10.1080/19420862.2015.1054585.
 35. Jain T, Sun T, Durand S, Hall A, Houston NR, Nett JH, Sharkey B, Bobrowicz B, Caffry I, Yu Y, et al. Biophysical properties of the clinical-stage antibody landscape. *Proc Natl Acad Sci USA.* 2017;114:944–49. doi:10.1073/pnas.1616408114.
 36. Proetzel G, Wiles M, Roopenian D. Genetically engineered humanized mouse models for preclinical antibody studies. *BioDrugs.* 2014;28:171–80. doi:10.1007/s40259-013-0071-0.
 37. Andersen J, Daba M, Berntzen G, Michaelsen T, Sandlie I. Cross-species binding analyses of mouse and human neonatal Fc receptor show dramatic differences in immunoglobulin G and albumin binding. *J Bio Chem.* 2010;285:4826–36. doi:10.1074/jbc.M109.081828.
 38. Magistrelli G, Malinge P, Anceriz N, Desmurs M, Venet S, Calloud S, Daubeuf B, Kosco-Vilbois M, Fischer N. Robust recombinant FcRn production in mammalian cells enabling oriented immobilization for IgG binding studies. *J Immunol Methods.* 2012;375:20–29. doi:10.1016/j.jim.2011.09.002.
 39. Petkova A, Sproule C, Khabbaz A, Brown P, Meng R. Enhanced half-life of genetically engineered human IgG1 antibodies in a humanized FcRn mouse model: potential application in humorally mediated autoimmune disease. *Int Immunol.* 2006;18:1759–69. doi:10.1093/intimm/dxl110.
 40. Avery L, Wang M, Kavosi M, Joyce A, Kurz J, Fan -Y-Y, Dowty M, Zhang M, Zhang Y, Cheng A, et al. Utility of a human FcRn transgenic mouse model in drug discovery for early assessment and prediction of human pharmacokinetics of monoclonal antibodies. *mAbs.* 2016;8:1–15. doi:10.1080/19420862.2016.1193660.